ELSEVIER

Biochimica et Biophysica Acta 1231 (1995) 58–68

BBA Biochimica et Biophysica Acta

# Initial spectroscopic characterization of the ciliate photoreceptor stentorin

Renke Dai [a], Tomoko Yamazaki [b], Iwao Yamazaki [b], Pill-Soon Song [a,*]

[a] *Department of Chemistry, University of Nebraska, Lincoln, NE 68588-0304, USA*
[b] *Department of Chemical Process Engineering, Hokkaido University, Sapporo 060, Japan*

Received 13 February 1995; accepted 31 March 1995

**Abstract**

Stentorin serves as the primary photosensor in the single cell ciliate, *Stentor coeruleus*, for its photophobic and phototactic responses to light of visible wavelengths. We separated two subunits, stentorin-2A and -2B, from the previous stentorin complex ('stentorin-2') of greater than half a million molecular mass isolated from the photoreceptor organelle (pigment granule). Stentorin-2B bears the chromophore covalently linked to an approx. 50 kDa apoprotein, as determined by SDS-urea-PAGE. Partial amino acid sequences were obtained from this 50 kDa subunit. Its visible and CD spectra were found to be similar to those of stentorin-2. The steady-state and time-resolved fluorescence spectra of stentorin-2B, in $H_2O$ and $D_2O$ buffers, were also similar to those of stentorin-2. This suggests that the 50 kDa subunit retains the spectral integrity and primary photoreactivity of the stentorin-complex. The picosecond time-resolved fluorescence study revealed that the short picosecond emission component ($\tau_F \cong 8-10$ ps) was the predominant emitting species in stentorin-2B and -2, followed by longer decaying species. No deuterium solvent effect was seen in this fast-decaying species. The possible mechanism for the primary photoreaction appears to involve electron transfer coupled with proton transfer.

*Keywords:* Photoreceptor; Stentorin ciliate; Photosensory transduction; Photophobic response; (*S. coeruleus*)

## 1. Introduction

*Stentor coeruleus* is a blue-green ciliated protozoan that exhibits step-up photophobic and negative phototactic responses to visible light [1,2]. The action spectra for the photoresponses are consistent with the absorption spectra of the pigment protein stentorin [1–4]. The structure (**1** or **2**, Scheme 1) of the stentorin chromophore was recently elucidated and shown to be a derivative of hypericin **3**; [5]. Structure 1 turned out to be the actual structure by total synthesis (Cameron, D., personal communication, 1994) and by a CD study [6].

Two chromatographically different species of stentorin can be obtained from the crude cell extract, stentorin-1 and -2 [7,8]. Stentorin-1 (ST-1) shows spectroscopic properties resembling those of the free chromophore of stentorin [8,9,6]. In contrast to ST-1, the stentorin-2 complex (ST-2) that can be detergent-solubilized from the pigment granules is only very weakly fluorescent, apparently due to a primary photoprocess in the picosecond time-scale [10,9]. However, rhodopsin-and phytochrome-like photochemical and thermal pathways, as detected by spectrophotometry under freeze-thaw cycling conditions, have not yet been demonstrated for stentorins.

Proton transfer in the excited state of ST-2 has been suggested as a possible primary photoprocess in triggering the light signal transduction chain in *Stentor* [11,12,10]. To further investigate the spectroscopic properties and photochemical reactivities of stentorin, we isolated the chromophore-bearing subunit (ST-2B) from the ST-2 complex. This complex also contains a non-chromophoric subunit (ST-2A) and, possibly, bound detergents [8]. We

Abbreviations: BA, benzylamine-agarose; BSA, bovine serum albumin; CD, circular dichroism; CHAPS, 3[(3-cholamidopropyl)dimethylammonio]-1-propanesulfonate; DEAE, diethylaminoethyl; DMSO, dimethyl sulfoxide; DTT, dithiothreitol; fwhm, full width at half maximum; FPLC, fast protein liquid chromatography; HA, hydroxylapatite; IEF, isoelectric focusing; PAGE, polyacrylamide gel electrophoresis; PMSF, phenylmethanesulfonyl fluoride; PVDF, poly(vinylidene difluoride); SDS, sodium dodecylsulfate; ST-2, stentorin-2; ST-2B, stentorin-2B; HO-ST-OH, stentorin; O = ST = O, oxy-stentorin; TCA, trichloroacetic acid.

* Corresponding author. E-mail: pssong@unl.edu; Fax: +1 402 4722044.


*SSDI* 0005-2728(95)00056-9

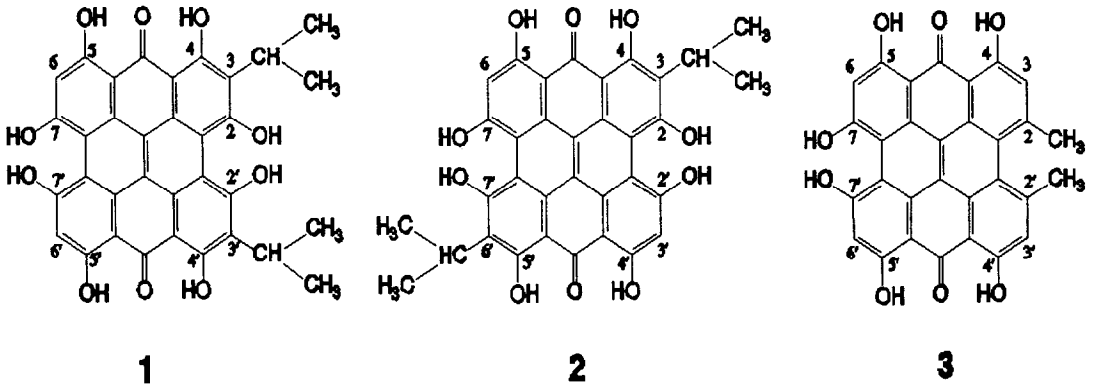

Scheme 1.

report here our initial characterization and fluorescent spectroscopic studies of stentorin-2B.

## 2. Materials and methods

### 2.1. Chemicals

Chemicals used in electrophoresis were electrophoresis grade from Bio-Rad (Richmond, CA). Other reagents used were purchased from Sigma Chemical Co. (St. Louis, MO) unless noted otherwise. All solutions were prepared using doubly deionized water ($ddH_2O$).

### 2.2. Preparation of stentorin extract

The isolation of ST-2B was based on a modification of the method developed by Kim [8]. The *Stentor* cells harvested were centrifuged at 3,000 g for 30 min at room temperature. Approx. 1.5 g of wet cell pellet was used per isolation. Approx. 8 mL of extraction buffer was added for each gram of wet pellet. The extraction buffer contained 20 mM Tris (pH 7.8), 2% CHAPS, 20% sucrose, 1 mM EDTA, 1 mM DTT (Bio-Rad) and 0.5 mM PMSF. This suspension was first sonicated for 5 min in an ice bath. The solution was then shaken for 30 min at 4°C, followed by centrifugation at $30000 \times g$ for 60 min. The supernatant was used as the ST-2 crude preparation. The remaining pellet was re-extracted with the same amount of extraction buffer. The suspension was sonicated for 1 min, shaken for 60 min and then centrifuged under the same conditions. Both supernatants were combined and subjected to column chromatography.

### 2.3. FPLC and column chromatography

The FPLC system used comprised an ISCO model 2360 gradient programmer, a model 2350 HPLC pump, an UV-5 multiple absorbance detector (ISCO, Lincoln, NE), a 50 mL superloop (Pharmacia, Piscataway, NJ) and home packed adjustable columns (Amicon, Beverly, MA). Absorbances at 280 nm and 620 nm were simultaneously monitored. The flow rate was controlled at 2 mL/min, except for the Bio-Gel column, which was eluted at 0.8 mL/min. All columns used were pre-equilibrated with the respective starting buffer.

Elution buffer A contained 20 mM Tris (pH 7.8), 0.05% CHAPS, 1 mM EDTA and 1 mM DTT. Approx. 18 mL of crude stentorin extract was applied to a G-15 column (2.2 (i.d.) × 18 (length) cm) and eluted with elution buffer A. The pooled stentorin fractions from the G-15 column (approx. 20 mL) were loaded onto a hydroxyapatite (HA) (Calbiochem, La Jolla, CA) column (2.2 × 15). Stentorin-1 was eluted with elution buffer A. Buffer A containing 0.5% CHAPS was then applied to the HA column to elute trace ST-1remaining on the column, stentorin-2 was eluted from the HA column with buffer B, containing 0.2 M phosphate buffer (pH 7.8), 0.7% CHAPS, 0.3% octyl glucoside, 1 mM EDTA and 1 mM DTT. Approximately 18 mL of ST-2 was collected from the HA column and then loaded onto a Bio-Gel A1.5 (Bio-Rad) column (2.5 × 50). The Bio-Gel column was washed with buffer A, and ST-2 eluted near the void volume. The ST-2 solution eluted from the Bio-Gel column was concentrated to less than 15 mL using a Centriprep 10 concentrator (Amicon) and further purified on a benzylamine-agarose (BA) hydrophobic interaction column (2.2 × 12). The following buffers were used for BA column: Buffer C, containing 20 mM Tris (pH 7.8), 1 mM EDTA, 1 mM DTT and 1 M NaCl; Buffer D, containing 20 mM Tris (pH 7.8), 1 mM EDTA and 1 mM DTT; and Buffer E, containing 20 mM Tris (pH 7.8), 1% octyl glucoside, 1% CHAPS, 1 mM EDTA and 1 mM DTT. The BA column was pre-equilibrated with buffer C. The concentrated ST-2 preparation was loaded onto the BA column, which was washed with buffer C for 3 min, followed by a linear gradient from buffer C to buffer D for 5 min. Buffer D was used to elute the stentorin-2A fraction. Stentorin-2B was eluted with buffer E. Phosphate buffer (20 mM, pH 7.8), instead of 20 mM Tris buffer, can also be used in buffers C, D and E. Samples in Tris buffer were freshly prepared for spectroscopic measurements and were stored at 6 ± 2°C. Sten-

torin-2B in phosphate buffer was stored at −20°C, or in solid $CO_2$ before use.

Stentorin solutions in $D_2O$ were prepared by buffer exchanges using a Centricon 10 (Amicon) concentrator. The sample solution was concentrated to approx. 0.15 mL. 2 mL of deuterated buffer (p*D* 7.8) was then added and the solution was concentrated again. This was repeated at least seven times for each sample. These preparations were performed at 4–8°C.

### 2.4. Protein concentration

The absorption maxima of ST-2 and -2B are red-shifted by approximately 12 nm relative to that of ST-1. Absorbances at the peak maxima of the fourth derivative spectra were monitored as a purity index for the ST-2 and -2B proteins during chromatographic purifications. Protein concentrations were determined with a Bio-Rad DC protein assay kit, according to the manufacturer's specifications. Hypericin was used in the control measurements to deduct possible interference by the chromophore in the calibration curve for the Bio-Rad DC protein concentration assay.

### 2.5. Sample preparation for gel electrophoresis

To prepare ST-2B for SDS-urea-PAGE, TCA was added to the ST-2B sample to give a final concentration of 10% TCA. Following incubation on ice for 1 h, the sample was centrifuged at 16000 × *g* for 20 min. The resulting pellets were washed with $ddH_2O$ and re-centrifuged. The pellets were then incubated while shaking in an electrophoresis sample buffer containing 2% SDS, 6 M urea and 0.375 M Tris (pH 6.8) for 10 h at room temperature. Following addition of solid DTT to a final concentration of 0.1 M, the samples were incubated for an additional 2 h. The solutions were then centrifuged at 16000 × *g* for 30 min; 20% glycerol (V/V) was added to the supernatant. Electrophoresis was then performed (described below). To prepare stentorin-2B for native-CHAPS-PAGE, concentrated ST-2B was mixed with an equal volume of 0.2 M Tris buffer (pH 6.8) containing 40% (v/v) glycerol.

### 2.6. Electrophoresis

SDS-urea-PAGE was performed according to the method of Laemmli [13] using 6 M urea and 3% sucrose in both 15% separating and 3.5% stacking gels. In addition, the running buffer also contained 2 M urea. Initially, a constant current of 10 mA was applied until all samples migrated into the stacking gel. The current was then increased to 20-30 mA.

For native-CHAPS-PAGE, SDS, DTT or mercaptoethanol were omitted from Laemmli's method. A 7.5% separating gel and a 3.5% stacking gel, both containing 0.5% CHAPS and 3% sucrose, were used. The running buffer also contained 0.5% CHAPS. As previously described, a constant current of 10 mA was applied until all samples migrated into the stacking gel and then the current was increased to 20–30 mA.

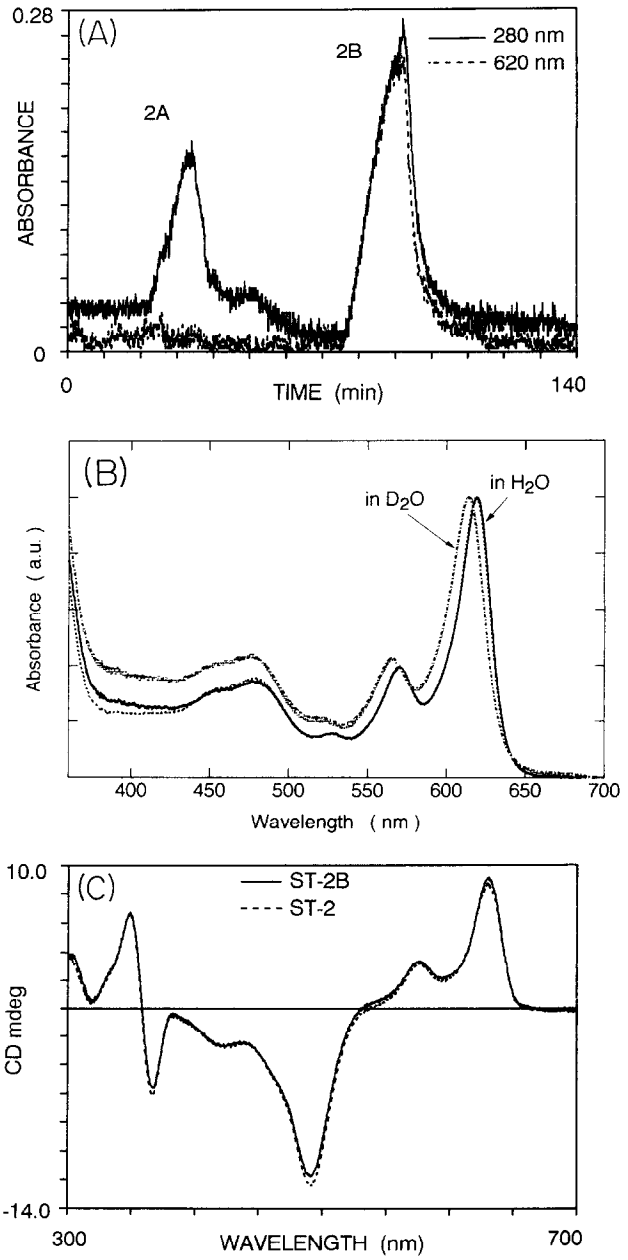


Fig. 1. (A) Elution profile on benzylamine-agarose, hydrophobic interaction column. Fraction ST-2A does not contain 620 nm absorption, while fraction ST-2B contains both 280 nm and 620 nm absorption. (B) Absorption spectra of stentorin-2 and ST-2B in $H_2O$-and $D_2O$-Tris buffer (pH 7.8). Peak maxima of stentorin-2 are 618.6 nm in $H_2O$ and 614.8 nm in $D_2O$ and those of ST-2B are 618.8 nm in $H_2O$ and 613.8 nm in $D_2O$. Absorbance was measured in a JASCO Ubest 50 spectrophotometer at room temperature. (C) CD spectra of ST-2B and stentorin-2 in Tris buffer (pH 7.8), which were measured by a JASCO J600 at room temperature.

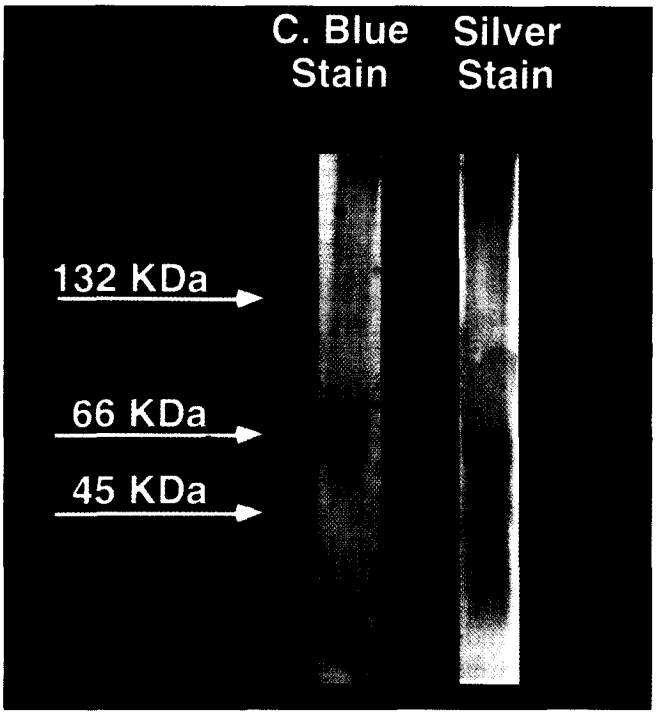


Fig. 2. Native-urea-PAGE of ST-2B in 7.5% gel with Coomassie Blue and silver stains. The molecular weight markers are albumin-chicken-egg (45000) and albumin-bovine (66000 and 132000, dimer) (Sigma).

### 2.7. Electrotransfer and microsequencing

Following SDS-urea-PAGE, the 50 kDa protein (ST-2B) was transferred to a PVDF membrane (Bio-Rad). The protein was electrotransferred at 30 V for 16 h at 6°C. Following transfer, the membrane was washed extensively with $ddH_2O$ for 48 h. The blue-green chromoprotein band was then excised and submitted to the Microchemistry Facility at Harvard University for the determination of amino acid composition and microscquencing after tryptic digestion. Amino acid sequencing of the N-terminal chain was unsuccessful, apparently because the N-terminus of the 50 kDa protein was blocked.

### 2.8. Time-Resolved fluorescence measurements

The procedures for measurement of fluorescence decays and time-resolved fluorescence emissions are described elsewhere [10,14]. The picosecond pulsed laser system consisted of a mode-locked Nd:YAG laser (Spectra Physics 3690) and a cavity-dumped rhodamine 6G laser (Spectra Physics 3500). The pulse width of the dye laser was approx. 2 ps (fwhm) and the intensity was 3.4 $mW/cm^2$ at 532 nm and at a 4 MHz repetition rate. The laser wavelength was 532 nm from the second harmonics of the Nd:YAG laser or 572–575 nm from the dye laser. The time-correlated single-photon-counting apparatus included a microchannel-plate photomultiplier (Hamamatsu R2809U-01), a time-to-amplitude converter (Ortec 457), a constant fraction discriminator (Tennelec TC454) and a multichannel pulse-height analyzer (Canberra 35 series). A pulse width of 30 ps (fwhm), the instrument response function, was measured for the scattered light from an aqueous vesicle solution. The decay curves were analyzed using a non-linear least-square iterative convolution method based on the Marquardt algorithm. The time-resolved fluorescence spectra were analyzed in terms of multiple emission components by using the Brand and Beechem globanal analysis routine [24], as adopted previously [14].

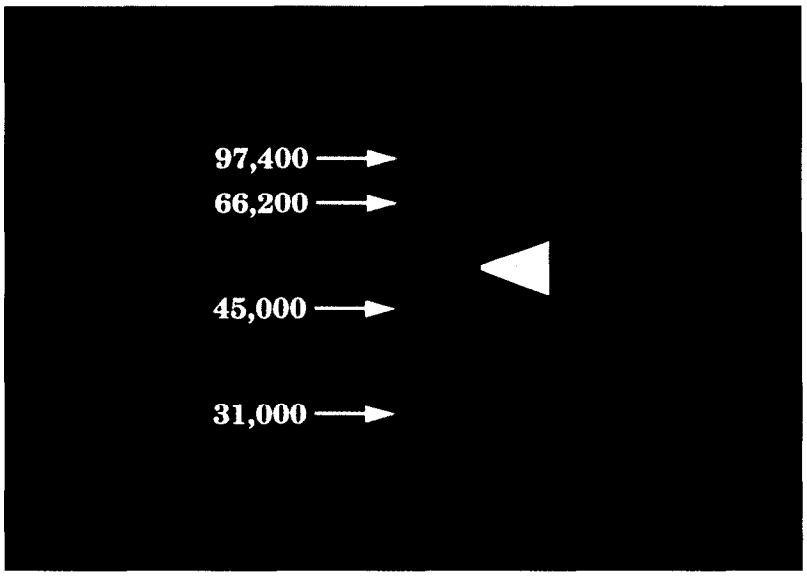


Fig. 3. SDS-urea-PAGE of ST-2B in 10% gel with Coomassie Blue stain. The MW markers are phosphorylase B-rabbit-muscle (97400), serum albumin-bovine (66200), ovalbumin-hen-egg-white (45000) and carbonic anhydrase-bovine (31000) (Bio-Rad).

## 3. Results

### 3.1. Stentorin characterization

Stentorin-2B was obtained by chromatography on HA and Bio-Gel columns in succession. The chromatographic elution profiles were similar to those previously published [8]. For the isolation of ST-2B as a chromophore-bearing subunit of the large complex (ST-2), the elution profile from the BA column is shown in Fig. 1A, with their absorbances monitored at 280 nm (due to protein plus chromophore) and 620 nm (due to chromophore only). Fractions containing ST-2A exhibit 280 nm absorption without significant 620 nm absorption. Fractions of ST-2B display both 280 nm and 620 nm absorbance.

Spectroscopic techniques were applied to investigate whether or not ST-2B retained the spectroscopic and photochemical integrity of stentorin as the photoreceptor molecule. Similar absorption spectra were obtained with the peak maxima at 618.8 nm for ST-2B and at 618.6 nm for ST-2 in $H_2O$-Tris buffer. Both exhibited absorption blue-shifts in deuterated Tris buffer with peak maxima at 613.8 nm for ST-2B and 614.8 nm for ST-2 (Fig. 1B). CD spectra of ST-2B and ST-2 were identical in $H_2O$-Tris buffer with the first and second peak maxima at 626.8 nm and 572.8 nm (Fig. 1C). For all practical purposes, the two species are spectroscopically indistinguishable. This indicates that the spectral integrity of ST-2B is preserved even when it is dissociated from the ST-2 complex. The purification factors were estimated to be approx. 85-fold according to the fourth-derivative spectra. The overall yield for ST-2B obtained from the post-G-15 column crude extract was approx. 1.5%.

### 3.2. Electrophoresis

The results from native-CHAPS-PAGE of ST-2B are shown in Fig. 2. Before Coomassie blue or silver staining, a blue-green band (the color of stentorin) was apparent on the gel. The molecular weight of ST-2B was estimated to be approx. 60000 in non-denatured PAGE. In SDS-urea-PAGE of ST-2B, a blue-green band was also seen on the gel without staining. The molecular weight of the blue-green band was estimated to be approx. 50000 (Fig. 3). Coomassie blue staining of the 50 kDa band was faint, apparently due to interference by SDS and urea.

Table 1
Amino acid composition analysis

| Amino acid | Composition pmol [a] | Percentage [a,b] |
|---|---|---|
| Asx (N, D) | 115.6 | 12.0 |
| Glx (Q, E) | 103.1 | 10.7 |
| Ser (S) | 64.8 | 6.7 |
| Gly (G) | 93.3 | 9.7 |
| His (H) | 10.5 | 1.1 |
| Arg (R) | 33.5 | 3.5 |
| Thr (T) | 43.0 | 4.5 |
| Ala (A) | 94.9 | 9.9 |
| Pro (P) | 39.9 | 4.1 |
| Tyr (Y) | 26.7 | 2.8 |
| Val (V) | 66.6 | 6.9 |
| Met (M) | 16.6 | 1.7 |
| Ile (I) | 59.5 | 6.2 |
| Leu (L) | 89.5 | 9.3 |
| Phe (F) | 48.8 | 5.1 |
| Lys (K) | 56.6 | 5.9 |

[a] The same ST-2B for microsequencing.
[b] Without consideration of tryptophan and cysteine.

### 3.3. Amino acid analysis

The amino acid composition of the 50 kDa band from SDS-urea-PAGE of ST-2B is shown in Table 1. Since the N-terminus of ST-2B was blocked, two fractions were collected by trypsin mapping and subjected to microsequencing. The resulting sequences were (1) NPFTAEL-VETA and (2) SILAADEVTGTIG.

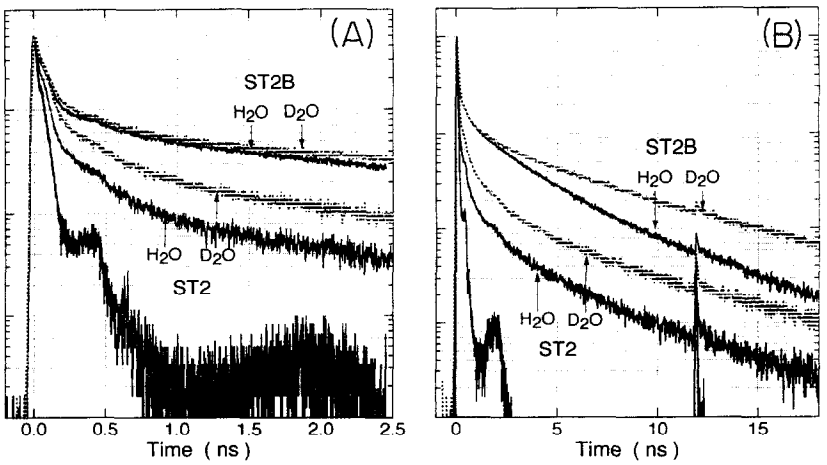


Fig. 4. Fluorescence decay curves of stentorin-2 and -2B at room temperature detected (A) at 630 nm in $H_2O$ or at 625 nm in $D_2O$ and (B) at 670 nm in $H_2O$ or 665 nm at $D_2O$. Excitation wavelength is 532 nm and time/channel corresponds to 2.64 ps (A) and 20.3 ps (B). The excitation curve is a instrumental response function measured with the laser scattered light.

Table 2
Time resolution, ps/ch, fluorescence lifetimes, $\tau_i$, related amplitudes (a) and $\chi^2$ for ST-2B and -2

| Temp. | Stentorin | Solvent | nm | ps/ch | $\tau_1$ ps(a) | $\tau_2$ ps(a) | $\tau_3$ ps(a) | $\tau_4$ ps(a) | $\chi^2$ |
|---|---|---|---|---|---|---|---|---|---|
| R.T. | ST-2B | $H_2O$ | 630 | 2.642 | 8(0.953) | 150(0.28) | 2209(0.019) | | 1.06 |
| | | | | 20.333 | 14(0.923) | 191(0.45) | 1693(0.021) | 4940(0.11) | 1.23 |
| | | $D_2O$ | 625 | 2.642 | 14(0.917) | 182(0.55) | 2967(0.029) | | 1.19 |
| | | | | 20.333 | 17(0.904) | 221(0.058) | 1591(0.019) | 7106(0.020) | 1.06 |
| | ST-2 | $H_2O$ | 630 | 2.642 | 9(0.976) | 159(0.020) | 1390(0.004) | | 1.03 |
| | | | | 20.333 | 10(0.981) | 200(0.014) | 1107(0.004) | 4820(0.001) | 1.16 |
| | | | 670 | 20.333 | 10(0.954) | 152(0.035) | 1171(0.008) | 5726(0.004) | 1.48 |
| | | $D_2O$ | 625 | 2.642 | 9(0.961) | 164(0.031) | 1572(0.009) | | 1.18 |
| | | | | 20.333 | 10(0.960) | 198(0.031) | 1226(0.007) | 6463(0.002) | 1.33 |
| | | | 665 | 20.333 | 10(0.950) | 198(0.037) | 1301(0.010) | 6525(0.004) | 1.12 |
| 77 K | ST-2 | $H_2O$ | 630 | 2.642 | 62(0.638) | 259(0.295) | 1886(0.06) | | 1.27 |
| | | | | 20.333 | 84(0.720) | 310(0.210) | 1241(0.049) | 4350(0.022) | 1.15 |
| | | | 675 | 20.333 | | 219(0.582) | 1462(0.265) | 6641(0.153) | 1.14 |

### 3.4. Fluorescence emission

Fluorescence decays of ST-2B and ST-2 in $H_2O$-or $D_2O$-Tris buffer excited by 575-nm laser pulses are compared in Fig. 4. Modest solvent deuterium effects are seen in the decay curves for ST-2B and -2, especially in the slow, nanosecond decay region. Table 2 summarizes the emission lifetimes and amplitude data for ST-2B and -2. A resolution of 2.6 ps/channel and an emission of 630 nm yielded three emitting components, while 20.3 ps/channel resolution resulted in four emitting components; the former sets of data are more reliable in the short lifetime ($\tau_1$ and $\tau_2$), and the latter sets of data are reliable in the long lifetime ($\tau_3$ and $\tau_4$). First, we should note that the predominant fluorescence component of approx. 8 ps (up to 95% contribution to the total fluorescence) was observed for ST-2B in $H_2O$-buffer, while a lifetime of 9 ps with a relative amplitude of 98% was obtained for ST-2. On changing the solvent from $H_2O$ to $D_2O$, the apparent differences in the fast, picosecond decays appear to be within experimental error. On the other hand, there is a

Table 3
Isotope effects on fluorescence lifetimes of ST-2B and ST-2 *

| Stentorin | $\tau_{1D}/\tau_{1H}$ | $\tau_{2D}/\tau_{2H}$ | $\tau_{3D}/\tau_{3H}$ | $\tau_{4D}/\tau_{4H}$ |
|---|---|---|---|---|
| ST-2B | 1.36 | 1.18 | 1.30 | |
| | 1.21 | 1.10 | 0.94 | 1.44 |
| | 0.94 | 0.85 | 0.94 | 1.43 |
| Average | 1.17 | 1.04 | 1.06 | 1.44 |
| ST-2 | 1.36 | 1.06 | 1.20 | |
| | 1.00 | 1.03 | 1.13 | |
| | 1.00 | 0.99 | 1.11 | 1.34 |
| | 0.77 | 0.88 | 1.07 | 1.46 |
| Average | 1.03 | 0.99 | 1.13 | 1.40 |

* Data are from Table 2 corresponding to emission at 630 nm in $H_2O$ and at 625 nm in $D_2O$.

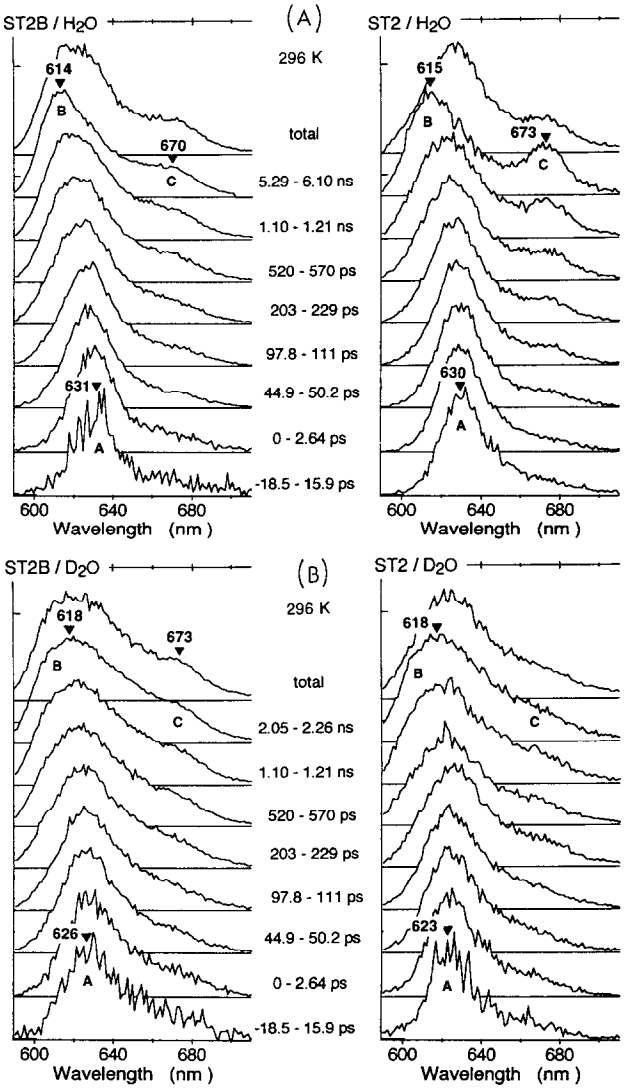


Fig. 5. Time-resolved fluorescence emission spectra with the comparison of stentorin-2 and ST-2B (A) in $H_2O$-and (B) in $D_2O$-Tris buffer at room temperature. The excitation wavelength is 572 nm and the time zero corresponds to the time in which the laser pulse reaches the maximum intensity.

discernible solvent deuterium effect on the slowest decay component of the fluorescence. To see the solvent deuterium effect, average values over the experimental fluctuation are listed in Table 3. It is seen that the lifetime is not affected by the deuterated solvent except for the longest lifetime component. These results were also observed with samples stored at 4°C.

Time-resolved fluorescence spectra of ST-2B and -2 are compared in both $H_2O$-and $D_2O$-Tris buffer at room temperature (Fig. 5). Non-exponential or multiple emission components are revealed in the time-resolved emission spectra. In ST-2B in $H_2O$, three emission bands appear: one centered at 631 nm (band A) in the initial time region (−18–50 ps), and after 2 ns, two at 614 nm (band B) and 670 nm (band C). In ST-2B in $D_2O$, essentially similar spectral behavior is seen, but the band A is significantly blue-shifted (626 nm). We also note that the spectral and time behavior of ST-2B are essentially identical with those of ST-2, indicating that the 50 kDa subunit, isolated from ST-2, retains the spectral integrity and primary photoreactivity.

Excitation spectra, while monitoring at wavelengths of 610 nm and 630 nm, essentially matched the absorption spectra (data not shown). The spectra obtained by monitoring emission at 660 and 690 nm, however, showed two minor components at 607 and 670 nm which are different from the absorption spectrum. These minor contributions in longer-wavelength emission are responsible for the long lifetime species in the time-resolved spectra.

## 4. Discussion

The two peptide sequences obtained are insufficient to determine the possible homology of ST-2B to a known membrane protein. A computer search of the Swiss-Prot and Genembl databases using WORKSEARCH identified several proteins exhibiting high homology to the sequences of fragments (1) NPFTAELVETA and (2) SILAADEVTGTIG from ST-2B. Two highly homologous gene products from photoreceptor cells were among those identified. The first is the *Drosophila ninaC* protein containing 1,501 amino acid residues with domains homologous to protein kinase and myosin [15]. Results from the BESTFIT program revealed that the similarity of sequence 1 to $-H_{279}$PFLTELIENE$_{289}$-of *ninaC* is 73%, while its identity is 55%. This homologous fragment is located in the kinase domain$_{17-282}$. Furthermore, there is a total of 10.2% aspartic acid and glutamic acid residues in this kinase domain. The similarity of sequence 2 is 50% and the identity, 42% to $-K_{596}$VLAAILNIGNI$_{607}$-of *ninaC*. This region is located in the myosin domain$_{329-1053}$, which contains 13% of aspartic acid and glutamic acid residues.

Another homologous protein is a sodium-calcium exchanger from bovine rod photoreceptors [16]. Sequence 1 exhibits 60% similarity and 40% identity to $-Q_{995}$PLSLEWPET$_{1004}$-of this protein, while sequence 2 displays 75% similarity and 42% identity to $-V_{1056}$WWAHQVGETIG$_{1067}$-. This 1,199 amino acid protein contains 17% aspartic acid and glutamic acid residues. As shown in Table 1, ST-2B may contain up to 27% of both aspartic-acid/asparagine and glutamic-acid/glutamine residues. Stentorin-2B migrates towards the pH 3 region in isoelectric focusing (IEF) (Dai and Song, unpublished data), while ST-2 complex isolated from sucrose density gradient centrifugation shows a pI value of 5.1 on IEF [17]. The acidic nature of ST-2B is similar to the acidity of the above two proteins. The molecular weight of the sodium-calcium exchanger was calculated from its gene to be 130000; however, its molecular weight was estimated to be 220000 by SDS-PAGE [18,16]. This abnormal migration may result from interference by the sugar residues and the extremely acidic domain [16]. In contrast, ST-2 precipitated upon addition of 2% SDS with or without heating, while ST-2B exhibited only slight solubility in 2% SDS. In the SDS-PAGE of ST-2, the blue-green material remained in the sample well and no band was apparent when stained with Coomassie blue. In SDS-urea-PAGE of ST-2B, several bands were stained by Coomassie blue, including the ~50 kDa chromophore-bound band (Fig. 3).

In the picosecond fluorescence studies the non-exponential, or multi-exponential decays of ST-2B and -2, were observed in all analyses (Fig. 4 and Table 2). The short-lived fluorescence-emitting species (8–18 ps lifetime) of ST-2B and -2 were found to be predominant (> 90%) in either $H_2O$-or $D_2O$-Tris buffer. In contrast, the parent chromophore, hypericin, in aqueous solution containing 6–25% ethanol displayed an exponential decay with a lifetime of 3–5 ns [19]. Free stentorin chromophore and ST-1 in $H_2O$-Tris buffer (pH 7.8) exhibited a two-exponential component emission with 2.5 and 6.0 ns lifetimes [10].

The non-exponential or multi-exponential nature of the excited state decays in ST-2 is quantitatively conserved in lifetimes and their amplitudes for ST-2B. This suggests that the non-exponential, or multi-exponential decays, reflect the intrinsic dynamics of the ST-2 and ST-2B excited states and are not due to impurities. The picosecond pump-probe absorption difference studies of ST-2 were concordant with the non-exponential or multi-exponential fluorescence decays. Thus, an efficient initial photoprocess occurred in the excited state ST-2, since ST-2 evolves quickly into an electronic state with a lifetime of < 3 ps in transient absorption changes [9]. This does not appear in the free chromophore species and hypericin. Since the ST-2 solution did not produce singlet oxygen [20], intersystem crossing does not play a significant role in the fluorescence decay kinetics of ST-2 and ST-2B. Since the short fluorescence lifetime reflects an efficient primary photochemical process, we can conclude that ST-2B re-

tains the functional integrity and photoreactivity critical for the light signal transduction in *Stentor coeruleus*.

### 4.1. Solvent deuterium effect

Effect of solvent deuterium appears on the time-resolved fluorescence spectra (Fig. 5). These spectra show substantial blue-shifts in the main emission band A, indicating that the hydroxyl protons of the chromophore exchange with $D^+$. However, the fluorescence lifetime ratio, $\tau_{1D}/\tau_{1H}$, is close to unity (Table 3), indicating no significant solvent deuterium effect on the excited state dynamics. One can expect that the fluorescence lifetime of the deuterated chromophore to be longer than that of the undeuterated chromophore, if proton transfer dominates the excited state process. For example, in dihydroxyanthraquinone, partly similar to hypericin, the fluorescence lifetime is affected by deuteration in hydroxy group, i.e., $\tau_D/\tau_H = 3.3 \sim 3.7$. [21]. Thus, the present result suggests that the photoprocess in the ps time region is not proton transfer in ST-2B and -2. However, in the intramolecularly H-bonded molecules such as hypericin, the lack of a deuteration effect does not rule out ultrafast proton transfer [22,23], and further studies are warranted to elucidate the role of proton transfer in ST-2B.

Fig. 1B shows a 5 nm blue shift of the absorption spectrum of ST-2B (4-nm blue shift for ST-2). This suggests a subtle conformational change in the ground state, or the effect of deuteration of the chromophore hydroxyls on the absorption spectrum.

### 4.2. Fluorescence properties at 77 K

Fig. 6 shows the time-resolved fluorescence spectra of ST-2 in $H_2O$ at 77 K; compared to the room temperature

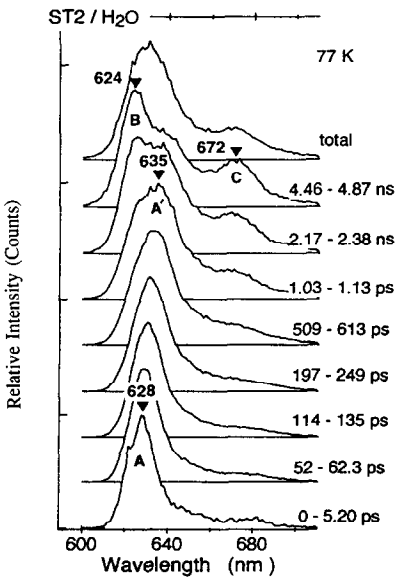


Fig. 6. Time-resolved fluorescence spectra of ST-2 in $H_2O$-buffer at 77 K. Excitation wavelength, 575 nm.

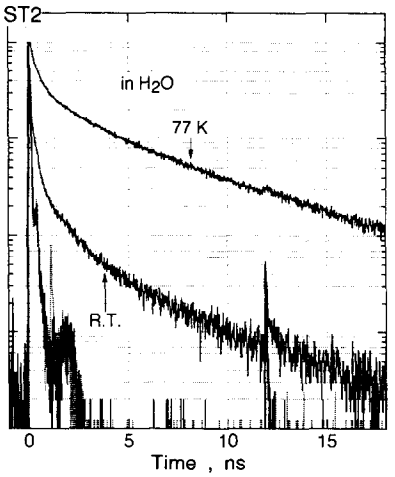


Fig. 7. Fluorescence decay curves of ST-2 in $H_2O$-phosphate buffer at room temperature and at 77 K. The excitation wavelength is 572 nm and the emission is monitored at 630 nm with 20.333 ps of time/channel. The time zero corresponds to the time in which the laser pulse reaches the maximum intensity. Multiple exponential decays occur at room temperature and exponential decay exists at 77 K in this particular ST-2 sample (see text for details).

spectra, the low temperature spectra show significant changes in spectral width and shift. The initial band at 628 nm (band A) is red-shifted to 635 nm (band A′) at 0–500 ps, and after 2 ns two bands appear at 624 nm (band B) and at 672 nm (band C). Similar spectral changes were also observed in $D_2O$ at 77 K. The peak position of band A′ at 634 nm is unchanged in $D_2O$, contrary to the other two components (bands A and B). This suggests that this species has no hydroxy protons that are exchangeable with $D^+$.

Fig. 7 shows the fluorescence decay at 77 K and room temperature. Similar decay curves were obtained with ST-2B (spectra not shown). The initial decay is much slower ($\tau_1 = 70$ ps) and the contributions of longer-decaying components are significantly enhanced relative to those at room temperature (Table 2). Note that there is no rise time in any of the decay curves at 77 K and room temperature. Thus, the spectral components shown above are unrelated to an excited state interconversion, and undergo relaxation independently of each other. Based on comparison of the time-resolved spectra at 77 K and room temperature, we assign bands A, B and C which appear at both 77 K and room temperature to the functional chromophore, the non-functional chromophore ST-1, and the excited state of an anionic stentorin present in the ground state (estimated at about 1% on the basis of deconvoluting its emission and excitation spectra), respectively.

We now consider the possible mechanisms for the primary photoreaction in the excited state of stentorin; chromophore conformation and local flexibility, proton transfer and electron transfer.

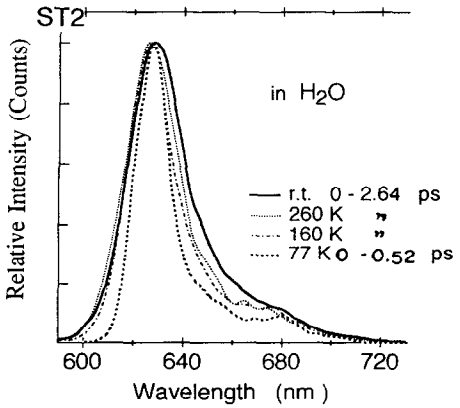


Fig. 8. Fluorescence spectra of ST-2 in $H_2O$/phosphate buffer taken from the spectra of an initial time region of the time-resolved spectra at different temperatures. Excitation wavelength is 575 nm.

### 4.3. Chromophore conformation and local flexibility

Fig. 8 shows fluorescence spectra of ST-2 in $H_2O$/phosphate buffer at different temperatures, which are taken from the spectra of an initial time region of the time-resolved spectra. It is seen that the spectrum becomes significantly sharp on decreasing temperature from room temperature to 77 K; the band width (fwhm) is 708 $cm^{-1}$ at room temperature and 421 $cm^{-1}$ at 77 K. The excitation spectra at 77 K and room temperature were similar and essentially matched the absorption spectra (data not shown). A sharpened fluorescence band at 77 K is 'mirror-image' to its absorption band. Similarly, in the case of ST-2B an fwhm of absorption band at 618.8 nm was 688 $cm^{-1}$ with an fwhm of 1281 $cm^{-1}$ for its fluorescence at room temperature, while an fwhm of 440 $cm^{-1}$ was found for the fluorescence at 77 K. A fluorescence fwhm for the free stentorin chromophore was found to be 456 $cm^{-1}$ at room temperature. The fluorescence behaviors of ST-2B and ST-2 at 77 K are similar to those of the free chromophore, and at least two fluorescence species ($< 620$ nm and $> 630$ nm) evolve when temperature is raised. As dynamic relaxation and photochemical processes accelerate in the excited state of stentorin at room temperature, the total fluorescence intensity of ST-2 is less than 2% of the free chromophore fluorescence [8].

As to the origin of the multi-exponential fluorescence decays in ST-2 and -2B at room temperature, we recall that single Trp-containing proteins exhibit non-exponential or multi-exponential fluorescence decays, arising from conformational heterogeneity, local motions and other photoprocesses [24]. Therefore, it is not unusual for the ST-2B with its covalently bound chromophore to exhibit multi-exponential or non-exponential fluorescence decays. What is unclear at the present is whether or not similar excited state dynamics account for the stentorin behavior. Time-resolved anisotropy studies, as applied to single Trp-containing proteins [25], will be helpful to resolve the motion dynamics of the chromophore from the non-exponential fluorescence behavior of stentorins.

### 4.4. Intermolecular and intramolecular proton transfer (tautomerism)

Based on ps pump-probe experiments, the $< 3$ ps transient absorption component has been interpreted as arising from intermolecular proton transfer to an appropriately situated amino acid residue on the ST-2 apoprotein [9]. On the other hand, an excited state tautomerism may play a significant role in the fluorescence decay dynamics in ST-2 and -2B. A recent study on hypericin ([22,23] and references therein) suggested that intramolecular proton transfer between two proton sites separated by only 2.5 Å occurs in subpicoseconds. Intramolecular proton transfer results in tautomerization of 7,14-dioxohypericin into 1,7-dioxo, 1,6-dioxo, or other tautomers. The 1,6-dioxo form is thermally stable at room temperature [26]. The absorption maximum of 1,6-dioxohypericin exhibited a 4-nm blue-shift in ethanol relative to 7,14-dioxo tautomer. Irradiation of 1,6-or 7,14-dioxohypericin in ethanol did not cause changes in their absorbance [26]. Thus, a primary step of photoreaction in ST-2 or -2B may be the formation of tautomers in subpicosecond time-scale, as has been proposed for hypericin [22]. The energy levels of the excited-state tautomers may be sufficiently close so that a thermal equilibrium among them is established within a subpicosecond time-scale at room temperature. Electron transfer may then follow in 8 ps at room temperature and in 70 ps at 77 K.

### 4.5. Electron transfer

Benzoquinone quenches the fluorescence of hypericin at a diffusion controlled rate [19]. The electron donor property of hypericin in its excited state can be reconciled with the results from the picosecond absorption difference measurements of hypericin [27], in which a new species is formed upon excitation in $\sim$ 5 ps with a transient absorption in the red/far-red region which was not present in the ground state absorption. Since this absorption can be faded by the electron scavenger solvent, acetone, it was further suggested that it arose from a solvated electron, as in photoionization processes in aqueous solution. Additionally, irradiation with light of longer than 520 nm produced an EPR-detectable free radical species from ST-2B in Tris buffer and the EPR signal decayed in the dark (Dai, Song and Golbeck, unpublished work). These observations provide supporting evidence that electron transfer plays a role in the excited state decays of stentorin. We suggest that electron transfer from the chromophore to a suitable acceptor/amino-acid residue (e.g., cystine) would quench the fluorescence of the excited state ST-2B and -2. The rate for this process can be estimated, using the short fluores-

cence decay lifetime, to be $\sim 1 \cdot 10^{11}$ $M^{-1}$ $s^{-1}$. This reaction is probably a reversible process.

To assess the possibility of a photoreaction cycle initiated by the primary electron transfer process, we investigated the photooxidation of hypericin in the presence of dithiodiethanol [28]. A redox potential of about +0.9 V for oxidation of hypericin was estimated from the cyclic voltammogram in DMSO [29]. The excited state redox potential for oxidation of hypericin could be enhanced by a difference of about 2 V [30]. Photooxidation of hypericin in the presence of DSDE ($HOCH_2CH_2$-S-S-$CH_2CH_2OH$) resulted in generation of mercaptoethanol (HS-$CH_2CH_2OH$) and oxidation of hypericin [28]. The redox potential for reduction of dithiodiethanol was predicted to be −0.95 V at pH 10 [31]. It is thus possible that photooxidation of stentorin (HO-ST-OH) produces a new quinone form as oxy-stentorin (O = ST = O);

$$HO - ST - OH + h\nu$$
$$\rightarrow HO - ST - OH^{*}$$
$$\rightarrow HO - ST - OH^{\cdot +} \rightarrow O = ST = O + 2H^{+}$$

Two electrons and two protons result from these reactions and could function to reduce the suitable amino acid residue(s), such as cystine, through the electron and proton transfer network. The potential for oxidation of mercaptoethanol is +0.02 V at pH 8 [31], while a potential of +0.6 V was reported for reduction of oxy-hypericin in DMSO [29]. Thus, the oxy-stentorin can be reduced back to stentorin to complete the photo-cycle. The redox potential for the cysteine-cystine system was estimated to be −0.21 V at pH 7.0 [32]. It is likely that the photooxidation of hypericin, and possibly stentorin, is more favorable in the cysteine-cystine system than in the dithiodiethanol-mercaptoethanol system. The primary photoreaction can then lead to the generation of a transient intracellular pH change across the pigment granular membrane in the signal transduction cascade in *S. coeruleus*.

## 5. Conclusions

The 50 kDa chromoprotein (ST-2B) was isolated from the large stentorin complex (ST-2). ST-2B displays fluorescence properties, visible CD and absorption spectra similar to those of ST-2. Therefore, ST-2B retains the spectral integrity and possibly the functional reactivity as photosensor in *S. coeruleus*. We suggest that a photo-cycle initiated by electron transfer is operative in ST-2B and ST-2. The fluorescence emissions of ST-2B and ST-2, commonly exhibit a fast decay ($\tau_F = 8 \sim 11$ ps) as the dominant fluorescence component. From the deuterium solvent effect and a comparison of the time-resolved fluorescence at room temperature with those at 77 K, it is concluded that the primary photoprocess in stentorin, corresponding to the fast fluorescence decay, is electron transfer. The electron transfer may take place from a tautomeric isomer resulting from the subpicosecond intramolecular proton transfer. Finally, we suggest that a photocycle initiated by electron transfer is operative in ST-2 and -2B, which may be coupled to a signal-transducing $\Delta pH_i$ in the ciliate cell.

## Acknowledgements

This work was supported by the U.S.P.H.S. NIH (R01-NS15426) and the Army Research Office (28748-LS-SM). The authors wish to thank the Dean of the College of Art and Sciences at the University of Nebraska for financing the printing of the color slide in this paper.

## References

[1] Song, P.-S., Häder, D.-P. and Poff, K.L. (1980) Arch. Microbiol. 126, 181–186.
[2] Song, P.-S., Häder, D.-P. and Poff, K.L. (1980) Photochem. Photobiol. 32, 781–786.
[3] Wood, D.C. (1976) Photochem. Photobiol. 24, 261–266.
[4] Fabczak, S., Fabczak, H., Tao, N. and Song, P.-S. (1993) Photochem. Photobiol. 57, 696–701.
[5] Tao, N, Orlando, M., Hyon, J.-S., Gross, M. and Song, P.-S. (1993) J. Am. Chem. Soc. 115, 2526–2528.
[6] Tao, N. (1994) Ph.D. Dissertation, University of Nebraska, Lincoln, NE.
[7] Walker, E.B., Lee, T.Y. and Song, P.-S. (1979) Biochim. Biophys. Acta 587, 129–144.
[8] Kim, I.-H., Rhee, J.S., Huh, J.W., Florell, S., Faure, B., Lee, K.W., Kahsai, T., Song, P.-S., Tamai, N., Yamazaki, T. and Yamazaki, I. (1990) Biochim. Biophys. Acta 1040, 43–57.
[9] Savikhin, S., Tao, N., Song, P.-S. and Struve, W. (1993) J. Phys. Chem. 97, 12379–12386.
[10] Song, P.-S., Kim, I.-H., Florell, S., Tamai, N., Yamazaki, T. and Yamazaki, I. (1990) Biochim. Biophys. Acta 1040, 58–65.
[11] Song, P.-S. (1981) Biochim. Biophys. Acta 639, 1–29.
[12] Song, P.-S. (1983) Annu. Rev. Biophys. Bioeng. 12, 35–68.
[13] Laemmli, U.K. (1970) Nature 227, 680–685.
[14] Yamazaki, T., Yamazaki, I., Nishimura, Y., Dai, R. and Song, P.-S. (1993) Biochim. Biophys. Acta 1143, 319–326.
[15] Montell, C. and Rubin, G.M. (1988) Cell 52, 757-772.
[16] Reilander, R., Achilles, A., Friedel, U., Maul, G., Lottspeich, F. and Cook, N.J. (1992) EMBO J. 11, 1689–1695.
[17] Walker, E.B. (1980) Dissertation, Texas Tech University, Lubbock, TX.
[18] Cook, N. J. and Kaupp, U. B. (1988) J. Biol. Chem. 263, 11382–11388.
[19] Yamazaki, T., Ohta, N., Yamazaki, I. and Song, P.-S. (1993) J. Phys. Chem. 97, 7870–7875.
[20] Dai, R., Song, P.-S., Anderson, J.L., Selke, M. and Foote, C.S. (1992) Proceedings of the IUBMB Conference on Biochemistry and Molecular Biology of Diseases, Nagoya, Japan.
[21] Lin, S. and Struve, W.S. (1991) J. Phys. Chem. 95, 2251–2256.
[22] Gai, F., Fehr, M.J. and Petrich, J.W. (1994) J. Phys. Chem. 98, 5784–5795.
[23] Gai, F., Fehr, M.J. and Petrich, J.W. (1994) J. Phys. Chem. 98, 8352–8358.
[24] Beechem, J. M. and Brand, L. (1985) Annu. Rev. Biochem. 54, 43–71.
[25] Tanaka, F. and Mataga, N. (1992) in Dynamics and Mechanisms of

Photoinduced Electron Transfer and Related Phenomena (Mataga, N., Okada, T. and Masuhara, H., eds.), pp. 501–512, North-Holland, Amsterdam.
[26] Etzlstorfer, C., Falk, H. and Oberreiter, M. (1993) Monatsh. Chem. 124, 923–929.
[27] Gai, F., Fehr, M.J. and Petrich, J.W. (1993) J. Am. Chem. Soc. 115, 3384–3385.
[28] Dai, R. (1994) Ph.D. dissertation, University of Nebraska-Lincoln, NE.
[29] Redepenning, J. and Tao, N. (1993) Photochem. Photobiol. 58, 532–535.
[30] Chanon, M., Hawley, M.D. and Fox, M.A. (1988) in Photoinduced Electron Transfer, Part A: Conceptual Basis (Fox, M.A. and Chanon, M., eds.), pp 1–59, Elsevier, New York.
[31] Zagal, J.H. and Paez, C. (1989) Electrochim. Acta 34, 243–247.
[32] Cleland, W.W. (1964) Biochemistry 3, 480–482.